An efficient bifunctional electrocatalyst of phosphorous carbon co-doped MOFs

Li Du
South China University of Technology
Mengyuan Lv
South China University of Technology
Dandan Liu
South China University of Technology
Huiyu Song (hysong@scut.edu.cn)
South China University of Technology

Nano Express

Keywords: bifunctional catalyst, ORR, OER, MOFs, C/P co-doped

Posted Date: August 5th, 2020

DOI: https://doi.org/10.21203/rs.3.rs-17338/v3

Version of Record: A version of this preprint was published on August 24th, 2020. See the published version at https://doi.org/10.1186/s11671-020-03394-x.

Abstract

It is eager to develop high-performance and cheap bifunctional electrochemical catalysts for both of the ORR or OER for the energy crisis and environmental problems. Herein, we report a series of ZIF-derived Co-P-C co-doped polyhedral materials with a well-defined morphology. The optimized catalyst Co/P/MOFs-CNTs-700 exhibited favorable electrochemical activities with the lowest over potential of 420 mV to achieve the current density of 10 mA cm^{-2} for OER and the half potential of 0.8 V for ORR in 0.1 M NaOH. The performance can be well improved by doping phosphorous resource which greatly changed its morphology. Meanwhile, the doped carbon resources also improve the conductivity, which makes it a promising bifunctional electrochemical catalyst and can be comparable with the commercial electrocatalysts.

Introduction

In recent years, the rapidly growing demand for energy sustainable development has drawn great interest among researchers in the field of electrochemical energy conversion and energy storage technologies[1-3]. In order to meet the demand for energy conversion and distribution, investigating an alternative non-precious metal electrode material with well-designed structure, controlled chemical and excellent electrochemical performance will be constant pursuit [4-7]. The oxygen evolution reaction (OER) and the oxygen reduction reaction (ORR) are the important reactions which act as significant roles in the application in solar cells, electrolysis cells, rechargeable metal-air cells, fuel cells and so on [8-11]. Nevertheless, the dull kinetic of OER and ORR severely limited the large-scale utilization of the energy conversion efficiency [8, 12-15].

Therefore, great efforts have been put to explore an efficient and stable electrochemical catalyst to improve the severe oxygen reaction in the past decades. It is known that the noble metal catalysts are the benchmark of the oxygen reaction. However, these prospective materials are suffered from scarcity, high cost and low stability. For example, iridium dioxide and ruthenium dioxide, the most promising OER catalysts, exhibit excellent OER electrocatalytic activities both in acidic and alkaline conditions at low over potential but still lacking long-term stability. The commercial platinum carbon catalyst as a kind of cathode electrocatalyst with the brilliant electrochemical activity of ORR is still cross-affected by the electrolyte, easy to be poisoned and lacks certain durability. Consequently, due to above shortcomings of the precious catalysts, more and more researchers have devoted to the design of electrochemical catalysts based on the abundant elements on the earth for the sustainable development. Interestingly, metal organic framework materials (MOFs) have attracted tremendous interests due to its low cost, abundant sources and the ability to serve as templates for the synthesis of carbon-based nanoporous materials. The crystalline porous materials MOFs are usually easy to design forming by self-assembly of metal ions and organic groups [16, 17]. The carbon-metal complexes derived from them can possess different morphology, exhibiting extremely high surface areas and hierarchical pore structures which contribute greatly to the electrochemical activities of ORR and OER [18, 19]. Nonetheless, the graphitization degree of these materials is relatively low, thus reducing the conductivity of the materials.

Meanwhile, carbon nanomaterials due to their high conductivity and controllable morphology are extremely attractive and have been applied in many electrochemical devices, such as polymer fuel cell [2, 20]. Moreover, it has been proved that carbon nanomaterials doped with heterogenous elements can greatly enhance the catalytic activity and the surface chemistry area [4, 13, 20-26]. The hetero-doped carbon materials also have synergistic effect in direct catalysis of ORR [27, 28]. Therefore, in order to enhance the conductivity and catalytic activity of the materials, it is reasonable to synthesize an efficient heterogenous atom doped materials from inexpensive source-rich materials MOFs, which can be well applied in fuel cells, metal-air batteries and so on.

Therefore, we report an efficient bifunctional electrochemical catalyst of the metal-organic framework with phosphorus and carbon co-doped by an in-situ doping method. We have found that doping heterogenous atom can change its morphology and improve the conductivity proved by SEM and XPS, which made it process a favorably low over potential of 420 mV to achieve the current density of 10 mA cm^{-2} for OER and the half potential of 0.8 V for ORR in 0.1 M NaOH. This promising bifunctional electrochemical catalyst can be comparable with the commercial electrocatalysts.

Methods

Synthesis of Co-MOFs carbon nanomaterials

In order to synthesize the Co-MOFs carbon nanomaterials, a typical and simple method was carried out as follows. Firstly, 1.28 g 2-Methylimidazole was ultrasonically dispersed in 20 mL methanol to form solution A. 1.0 g Cobalt (II) acetylacetonate was ultrasonically dispersed in 60 mL methanol to form solution B. The solution A was slowly added into solution B with continually ultrasonic for 5 minutes, followed by vigorous stirring for another 10 minutes at room temperature. Then the mixture was sealed in the polytrafluoroethylene reactor, which was transferred into the air-dry oven and heated from room temperature to 160 °C and maintained at 160 °C for 24 h, followed by naturally cooling down to room temperature. The obtained purple solid powder was centrifuged and washed with methanol for several times and dried at 70 °C overnight. The prepared nanocrystals were pyrolyzed under an argon atmosphere in a flow-through quartz tube placed in the center of a tube furnace as follows. Firstly, the production was heated from room temperature to 350 °C at a rate of 5 °C / min and maintained at 350 °C for 1 h. Then we increased it to the desired temperature (500,600,700,800 and 900 °C) for 2 h with the same heating rate to obtain Co-MOFs-x, where “x” represents the carbonization temperature.

Synthesis of Co/P-MOFs carbon nanomaterials

In order to figure out the impact of doping P on the electrochemical activities, different phosphine sources were adopted during the synthesis. 1.28 g 2-Methylimidazole was ultrasonically dispersed in 20 mL methanol to form solution A. 1.0 g Cobalt (□) acetylacetonate and 0.25 g phosphorus source were ultrasonically dispersed in 60 mL methanol to form solution B. The phosphorus sources were sodium

hypophosphite, triphenyl phosphine and O-trimethylphenyl phosphine. The following steps were the same as the above, we only changed the most suitable carbonization temperature as 700 °C. Finally, we obtained the productions named as Co/P0-MOFs, CoP1-MOFs and Co/P2-MOFs, where P0, P1 and P2 represents sodium hypophosphite, triphenyl phosphine and O-trimethylphenyl phosphine, respectively.

We chose the triphenyl phosphine as the phosphorus source and changed the mass of phosphorus source in step (1) to 0.5, 0.75 and 1.0 g, respectively. And the other experimental steps were unchanged. The final product was named Co/P/MOFs-700-0.25, Co/P/MOFs-700-0.5, Co/P/MOFs-700-0.75 and Co/P/MOFs-700-1.0, respectively.

Synthesis of Co-MOFs-C carbon nanomaterials

In order to improve the conductivity of the material, additional carbon sources were added. 1.28 g 2-Methylimidazole was ultrasonically dispersed in 20 mL methanol to form solution A. 1.0 g Cobalt (□) acetylacetonate and 0.125 g carbon sources were ultrasonically dispersed in 60 mL methanol to form solution B. The carbon sources were carbon nanotubes (CNTs), acetylene black (CB) and A-OMCS that were prepared in our formal article [25] which were acid treated. The following steps were the same as the step2.2 (1). Finally, we obtained the productions named as Co/MOFs-CNTs-700, Co/MOFs-CB-700 and Co/MOFs-A-OMCS-700, respectively.

Synthesis of Co/P-MOFs-CNTs-700 carbon nanomaterials

In order to improve the conductivity and electrocatalytic performance, carbon sources and carbon materials were used synchronously at one time. 1.28 g 2-Methylimidazole was ultrasonically dispersed in 20 mL methanol to form solution A. 1.0 g Cobalt(□) acetylacetonate, 0.25 g triphenyl phosphine and 0.125 g CNTs with acid treated were ultrasonically dispersed in 60 mL methanol to form solution B. The following steps were the same as the above. Finally, we obtained the productions named as Co/P/MOFs-CNTs-700.

Characterization of the synthesized carbon nanomaterials

X-ray diffraction (XRD) were carried out on TD-3500 (Tongda, China) diffractometer. X-ray photoelectron spectroscopy (XPS) was carried out using a photoelectron spectrometer K-Alpha+ (Thermo fisher Scientific). Scanning electron microscopy (SEM) images were obtained with an SU8220 scanning electron microscope (Hitachi, Japan). High-angle annular dark field (HAADF) imaging and energy-dispersive spectrometer (EDS) elemental mapping analysis were performed in the scanning transmission electron microscopy (STEM) mode on an aberration-corrected FEI Tecnai f20 field emission transmission the electron microscope operated at 200 kV.

Electrochemical Tests

All electrochemical activity data were collected on an electrochemical workstation (Ivium, Netherlands) at room temperature, coupled with a rotating disk electrode (RDE) system (Pine, USA) in a standard three-electrode system. The three-electrode system consisted of a Pt-wire counter electrode, a Hg/HgO (0.1 M NaOH solution) reference electrode for the alkaline medium and a glassy-carbon-based working electrode (GC, 0.196 cm^2). The catalyst-loaded electrodes were obtained as follows. Firstly, a catalyst ink was prepared by ultrasonicating a mixture of 1 mL of 0.25 wt % Nafion ethanol solution and 5 mg of the corresponding catalyst for 30 min. Then, 20 μL of catalyst ink was spread on a glassy-carbon-based working electrode in the RDE tests. Finally, the working electrode was dried under an infrared lamp for 1-2 min. The catalyst loading was approximately 0.5 mg cm^{-2}. A 0.1 M NaOH solution was employed as the electrolyte and was purged with high-purity N_2 or O_2 gas for about 30 min before testing. Linear sweep voltammetry (LSV) tests were performed at a rotation rate of 1600 rpm and a potential scan rate of 10 mV s^{-1}. Stability test was performed on Autolab Electrochemical Instrumentation (Metrohm) workstation in a standard three-electrode system, which OER was by chronopotentiometry test conducted under constant current density of 10 mA cm^{-2} in 0.1 M NaOH with a loading of 0.2 mg cm^{-2} and ORR was by chronoamperometric responses test performed under constant potential of 0.8 V under same condition. All potentials are calibrated with respect to the reversible hydrogen electrode (RHE).

Results And Discussion

As shown in Fig. 1a, X-ray diffraction (XRD) revealed that we have successfully synthesized polyhedrons of transition metal organic framework materials. When increasing the carbonization temperatures, the diffraction peaks at 44.216°, 51.522° and 75.853° become more distinct, which matches well with the (111), (200) and (220) planes of the cubic Cobalt (PDF#15-0806). As is known to all, the annealing temperature has significant effect on the physicochemical and electrochemical performance of the samples [29, 30]. Thus, the obtained samples with a series of temperature gradient were conducted electrochemical measurements to examine the optimized temperature. Fig. 1b shows the electrochemical activities of the materials treated at different temperatures. It is obvious to find that the as-prepared catalyst carbonized at 700 °C (Co/MOFs-700) exhibits the best OER performance. The overpotential is around 480 mV to achieve the current density of 10 mA cm^{-2} in 0.1 M NaOH.

Then the Co/MOFs before carbonized and the best performed Co/MOFs-700 were picked to carry out the SEM measurements. As shown in Fig. 1c and 1d, the morphology of the obtained Co/MOFs-700 has changed greatly after carbonized at 700 °C. Many fold-like lines appear on its surface and is not smoother than the original materials without carbonized. But it still processes the polyhedron morphology, with regular particle dispersion and no collapse sign.

As previous articles reported, doping the phosphor into transition metal organic framework polyhedron can increase the stability of the sample in acid or alkaline solution and can also effectively improve the

electrochemical catalytic activity by break the electroneutrality and facilitate of the O_2 adsorption to enhance the catalytic activity [31-33]. Therefore, phosphorus-doped samples are synthesized with in-situ doping method and investigated the electrochemical performance. The obtained products were named as Co/P0/MOFs-700, Co/P1/MOFs-700 and Co/P2/MOFs-700, while the P0, P1, P2 represents the phosphorus sources of sodium hypophosphite, triphenylphosphine and o-trimethylphenyl phosphine, respectively.

According to Fig. 2a, the diffraction peaks of the phosphorus-doped samples still possess the pattern of cubic Cobalt (PDF#15-0806), indicating that doping slight amount of phosphor would not change the structure of the MOFs. Then the electrochemical measurements were conducted to explore the influence of different phosphorus sources on electrochemical catalytic activities. As shown in Fig. 2c, the open potential (0.87 V) and half wave potential (0.78 V) both shows that the Co/P1/MOFs-700 possesses the best ORR activity. However, it is slightly weaker than that of the original product Co/MOFs-700 carbonized under the same temperature. Fig. 2d represents the OER performance of different products doped with phosphorus. When the limited current density is 10 mA cm^{-2}, only Co/P1/MOFs-700 owns the lowest over potential of 430 mV, demonstrating that incorporation of phosphorus into the samples can increase the OER activity, which is coincidence with the reported article that incorporation of phosphorus would adjust the electrical conductivity and meanwhile facilitate the rapid electrons transfer[34]. Moreover, Fig. 2b shows a comparison between the sample with triphenylphosphine as phosphorus source and the original sample (Fig 1c) without incorporation of elements. It can be revealed that the incorporation of phosphorus greatly affected the morphology of the material compared with Co/MOFs-700. Therefore, doping phosphor can not only enhance the electrochemical activity but also changed the morphology of the sample.

Subsequently, in order to further figure out the reason why doping phosphorus can enhance the electrochemical activity. XPS analysis were carried out to probe the composition and chemical state of the Co/MOFs-700 and Co/P1/MOFs-700 sample. According to Fig. 3a, XPS spectra survey of Co/MOFs-700 and Co/P1/MOFs-700 both shows the presence of Co 2p, O 1s, N 1s and C 1s. It is noted that the peak of P 2p appears in the XPS spectra survey in Co/P1/MOFs-700 but shows a rather weak signal compared with strong peaks of C 1s. Moreover, Fig. 3b shows the Co 2p spectra of Co/MOFs-700 and Co/P1/MOFs-700. It was found that the Co 2p 3/2 can be fitted into two peaks. The peaks located at 778.2° and 780.7° can be ascribed to the Co (0) and Co (2^+). While Co 2p 1/2 can also be displayed into two peaks positioned at 793.3° and 796.7°, which can be ascribed to the Co (0) and Co (2^+). The satellites peaks were positioned at 786.2° and 802.7° [35-37]. When compared with phosphorus-doped sample Co/P1/MOFs-700, we can find that the Co (0) were greatly increased while Co (2^+) decreased, indicating that doping phosphorus source during the synthesis process can increase the content of Co (0) in the obtained samples. As is known to us all, Co (0) can greatly enhance the conductivity, thus improve the electrochemical performances which also in accordance with the previous report [38].

Afterwards, we continued to investigate influence on the quality of the doped phosphorus source. The obtained products with a different molar ratio of P were named as Co/P/MOFs-700-x (x = 0.25, 0.5, 0.75, 1.0), while P represents triphenylphosphine and x represents the quality of phosphorus source. Fig. 4a shows that when increasing the content of phosphorus sources, the XRD pattern shows that the main diffraction peaks in these samples are still Cobalt (PDF#15-0806). As Fig. 4b shows, Co/P/MOFs-700-0.5 possesses the best ORR activity whose half wave potential was around 0.8 V among these phosphorus-doped products, but the ORR activity of Co/P/MOFs-700-0.5 is not increased significantly compared with the original sample Co/MOFs-700. It can be seen from Fig. 4c that the OER activity of the samples increased significantly with the addition of triphenylphosphine compounds and decreased with the increase mass of phosphorus source. When the limited current density is 10 mA cm^{-2}, Co/P/MOFs-700-0.25 and Co/P/MOFs-700-0.5 both own the minimum overpotential of 450 mV, indicating that only proper amount of phosphorus sources can improve OER activity while the amount of 0.25 and 0.5 exhibit best. However, when compared with commercial platinum carbon (half-wave potential 0.81 V, limiting current density 5.43 mA cm^{-2}) and excellent OER electrocatalysts Iridium oxide (1.61V @ 10 mA cm^{-2}), Co/P/MOFs-700-0.5 still remains significant difference among the limited current density in ORR performance. As the article reported, when the conductivity of the material is small, so is the limited current density [39].

In order to enhance the conductivity, we firstly measured the current carbon content of the synthesized Co/P/MOFs-700-0.5 analyzed by EDS images. According to Fig. 5, it is obvious that the quality of cobalt accounts for the most which takes almost 52.38%, while the quality of carbon is relatively less of 29.13%.

Therefore, in order to improve the conductivity of the material, we further doped the samples with carbon without any phosphorus sources. The obtained products were named as Co/MOFs-CNTs-700, Co/MOFs-CB-700 and Co/MOFs-A-OMCS-700, respectively. Fig. 6a shows that doping carbon will not affect the structure of the samples, which still keeps the same diffraction peaks of Cobalt (PDF#15-0806). As shown in Fig. 6b, it can be seen that the limited current density of the products are greatly increased with the incorporation of carbon source in ORR, while Fig. 6c indicated that the incorporation of carbon source makes no sense to improve the OER properties of the catalysts.

Combined with the previous experimental data and conclusions, we doped the original sample with both phosphorus and carbon elements by adding 0.5 g of triphenylphosphine and a suitable amount of different carbon sources (CNTs, CB and A-OMCS) to the material for comparison. The obtained samples were named as Co/P/MOFs-CNTs-700, Co/P/MOFs-CB-700 and Co/P/MOFs-A-OMCS-700, respectively. According to Fig. 7a, there is no change of the XRD pattern, with all the samples matching well with cubic Cobalt (PDF#15-0806). As shown in Fig. 7b, co-doping with phosphorus and carbon greatly increased the limited current density and ORR performance of the products. The sample of Co/P/MOFs-CNTs-700 exhibits the best ORR activity, which the half wave potential and limiting current density are 0.8V and 4.81 mA cm^{-2} and is 10 mV lower than that of commercial platinum carbon. Additionally, as can be seen clearly in Fig. 7c, the OER performance of the products have also been greatly improved. The sample of Co/P/MOFs-CNTs-700 exhibits the lowest over potential voltage of 420 mV. Compared with the voltage

corresponding to dioxide iridium, Co/P/MOFs-CNTs-700 is only about 40 mV higher than dioxide iridium. Therefore, Co/P/MOFs-CNTs-700 exhibits to be a favorable bifunctional electrocatalyst.

Meanwhile, to access the stability of the best performed Co/P/MOFs-CNTs-700, chronopotentiometry and chronoamperometric responses tests were carried out. As can be seen in Fig. 8a and 8b, the overpotential only increased 1.5 mV and the ORR performance are reduced by 79.5% after 18 hours continuous tests, proving that both OER and ORR activity of Co/P/MOFs-CNTs-700 are rather stable in 0.1 M NaOH.

Scanning electron microscopy, EDS and mapping on the sample of Co/P/MOFs-CNTs-700 have also been carried out. As can be seen from Fig. 9a-c, Co/P/MOFs-CNTs-700 retained the polyhedron morphology with many fold-like lines on the surface. Besides, the incorporation of carbon nanotubes is embedded into the skeleton of the product, which may increase the specific surface area of the product and provides more adsorption sites for electrochemical reaction. Fig.10d-g are the mapping analysis of the sample. It can be seen that the carbon and phosphorus sources are uniformly dispersed in the skeleton of the sample and become a whole.

As EDS shows, the content of phosphorus and carbon of the material is increased compared with the original sample of Co/MOFs-700 by in-situ doping, thus leading to the increased ORR and OER activity. It is laterally demonstrated that the incorporation of two kinds of phosphorus and carbon elements could be beneficial to increase the electrochemical activity of metal organic framework materials containing cobalt [40]. Because the electronegativity of P (2.19) is different from that of carbon atoms (C: 2.55). Co-doping would break the electroneutrality which can facilitate of the O_2 adsorption and improve the ORR activity [41]. Meanwhile, more active sites can arise due to the co-doping phosphorus and carbon by changing the asymmetric spin density of heteroatoms and effectively weak the O-O bonding, thus leading to the enhanced ORR activity [42].

The outstanding electrochemical activities can be attributed to the following reasons. Firstly, doping hetero atoms would lead to the redistribution of the charge density on the catalyst surface, which is beneficial to adsorb oxygen and promote the ORR activities [43]. Secondly, codoping different atoms into the MOFs would result in the synergistic effect which also contributes to the enhanced electeochemical performance [44]. Thirdly, it has been proved that the OER mechenism of Co-based catalyst is a dynamic surface self-reconstruction process. The Co atoms on the surface could form a self-assembled metal oxy(hydroxide) active layer of CoOOH which works as real active site [45]. In addition to the composition, the unique hybrid structure combined with its high conductivity could provide large surface area for the fast charge transfer.

Conclusion

In conclusion, an efficient and cost-effective polyhedron transition metal organic framework carbon nanomaterial (Co/P/MOFs-CNTs-700) co-doped with phosphorus and carbon sources have been successfully synthesized, which can serve as an efficient and cheap bifunctional electrochemical

catalyst. The lowest over potential of Co/P/MOFs-CNTs-700 is 420 mV to achieve the current density of 10 mA cm^{-2} for OER and the half potential is 0.8 V for ORR in 0.1 M NaOH, which is very close to those of commercial electrochemical catalysts. It could be utilized as a promising electrochemical bifunctional electrocatalyst in the energy storage field and also provide a promising insight to design electrochemical bifunctional electrocatalyst.

Declarations

Availability of data and material

The data used to support the findings of this study are included within the article.

Competing Interests

The authors declare that this work was conducted in the absence of any commercial or financial relationships that could be construed as a potential conflict of interest.

Founding

This work was supported by the National Key Research and Development Program of China (No. 2018YFB0105500).

Contributions

Li Du and Mengyuan Lv contributed equally to this work, in which Li Du provided the idea and Mengyuan Lv wrote this manuscript and performed the characterizations. Dandan Liu carried out the electrochemical experiments. Huiyu Song revised the manuscript. All authors read and approved the final manuscript.

Acknowledgements

We gratefully thank the XPS measurement from Shiyanjia Lab.

Abbreviations

ORR：Oxygen reduction reaction

OER：Oxygen evolution reaction

SEM：Scanning electron microscopy

HAADF：High-angle annular dark field

EDS：Energy-dispersive spectrometer

STEM：Scanning transmission electron microscopy

XPS：X-ray photoelectron spectroscopy

XRD：X-ray diffraction

RDE：Rotating disk electrode

Co-MOFs-x：Cobalt-metal organic frameworks-x represents temperature

Co/P-MOFs：Cobalt/phosphorus-metal organic frameworks

Co/P/MOFs-700-0.25：Cobalt/phosphorus-metal organic frameworks-700°C-the mass of phosphorus source is 0.25

Co-MOFs-C：Cobalt-metal organic frameworks-carbon

Co/P-MOFs-CNTs-700：Cobalt/phosphorus-metal organic frameworks-carbon nanotubes-700°C

GC：Glassy carbon

LSV：Linear sweep voltammetry

RHE：Reversible hydrogen electrode

Pt/C：Platinum/carbon catalyst

References

1. M. G. Walter, E. L. Warren, J. R. Mckone, S. W. Boettcher, Q. Mi, E. A. Santori and N. S. Lewis, "Solar water splitting cells," *Chemical Reviews*, vol. 110, no. 11, pp. 6446-6473, 2010.
2. J. Zhang, Z. Xia and L. Dai, "Carbon-based electrocatalysts for advanced energy conversion and storage," *Science Advances*, vol. 1, no. 7, pp. e1500564, 2015.
3. G. N. Nielson, M. Okandan and W. C. Sweatt, "Leveraging scale effects to create next-generation photovoltaic systems through micro- and nanotechnologies," *Proceedings of SPIE - The International Society for Optical Engineering*, vol. 8373, no. 12, pp. 1106-1112, 2012.
4. E. Proietti, F. Jaouen, M. Lefèvre, N. Larouche, J. Tian, J. Herranz and J. P. Dodelet, "Iron-based cathode catalyst with enhanced power density in polymer electrolyte membrane fuel cells," *Nature Communications*, vol. 2, no. 2, pp. 416, 2011.

5. R. V. Jagadeesh, A. E. Surkus, H. Junge, M. M. Pohl, J. Radnik, J. Rabeah, H. Huan, V. Schünemann, A. Brückner and M. Beller, "Nanoscale Fe_2O_3-based catalysts for selective hydrogenation of nitroarenes to anilines," *Science*, vol. 342, no. 6162, pp. 1073, 2013.
6. M. Sun, H. Liu, Y. Liu, J. Qu and J. Li, "Graphene-based transition metal oxide nanocomposites for the oxygen reduction reaction," *Nanoscale*, vol. 7, no. 4, pp. 1250-1269, 2015.
7. S. Yang, G. Cui, S. Pang, Q. Cao, U. Kolb, X. Feng, J. Maier and K. Müllen, "Fabrication of cobalt and cobalt oxide/graphene composites: towards high-performance anode materials for lithium ion batteries," *Chemsuschem*, vol. 3, no. 2, pp. 236-239, 2010.
8. L. Jörissen, "Bifunctional oxygen/air electrodes," *Journal of Power Sources*, vol. 155, no. 1, pp. 23-32, 2006.
9. G. Chen, D. A. Delafuente, S. Sarangapani and T. E. Mallouk, "Combinatorial discovery of bifunctional oxygen reduction - water oxidation electrocatalysts for regenerative fuel cells," *Catalysis Today*, vol. 67, no. 4, pp. 341-355, 2001.
10. D. Lee, B. Kim and Z. Chen, "One-pot synthesis of a mesoporous NiCo2O4 nanoplatelet and graphene hybrid and its oxygen reduction and evolution activities as an efficient bi-functional electrocatalyst," *Journal of Materials Chemistry A*, vol. 1, no. 15, pp. 4754-4762, 2013.
11. L. Qu, Y. Liu, J. B. Baek and L. Dai, "Nitrogen-doped graphene as efficient metal-free electrocatalyst for oxygen reduction in fuel cells," *ACS Nano*, vol. 4, no. 3, pp. 1321-1326, 2010.
12. J. Hou, Y. Shao, M. W. Ellis, R. B. Moore and B. Yi, "Graphene-based electrochemical energy conversion and storage: fuel cells, supercapacitors and lithium ion batteries," *Physical Chemistry Chemical Physics*, vol. 13, no. 34, pp. 15384-15402, 2011.
13. M Winter and R J. Brodd. “What Are Batteries, Fuel Cells, and Supercapacitors?” Cheminform, vol. 104, no. 10, pp. 4245-4270, 2004.
14. H. Gröger, "The development of new monometallic bifunctional catalysts with Lewis acid and Lewis base properties, and their application in asymmetric cyanation reactions," *Chemistry*, vol. 7, no. 24, pp. 5246-5251, 2001.
15. G. L. Tian, M. Q. Zhao, D. Yu, X. Y. Kong, J. Q. Huang, Q. Zhang and F. Wei, "Nitrogen-doped graphene/carbon nanotube hybrids: in situ formation on bifunctional catalysts and their superior electrocatalytic activity for oxygen evolution/reduction reaction," *Small*, vol. 10, no. 11, pp. 2251-2259, 2014.
16. D. W. Fu, W. Zhang and R. G. Xiong, "The first metal-organic framework (MOF) of Imazethapyr and its SHG, piezoelectric and ferroelectric properties," *Dalton Transitions*, vol. 30, no. 30, pp. 3946-3948, 2008.
17. M. J. Macleod and J. A. Johnson, "Block co-polyMOFs: assembly of polymer–polyMOF hybrids via iterative exponential growth and “click” chemistry," *Polymer Chemistry*, vol. 8, no. 31, pp. 4488-4493, 2017.
18. M. Zhang, Q. Dai, H. Zheng, M. Chen and L. Dai, "Novel MOF-Derived Co@N-C Bifunctional Catalysts for Highly Efficient Zn–Air Batteries and Water Splitting," *Advanced Materials*, vol. 30, no. 10, pp.

1705431, 2018.

19. D. Ji, S. Peng, L. Fan, L. Li, X. Qin and S. Ramakrishna, "Thin MoS_2 nanosheets grafted MOFs derived porous Co-N-C flakes grown on electrospun carbon nanofibers as self-supported bifunctional catalysts for overall water splitting," *Journal of Materials Chemistry A*, vol. 5, no. 45, pp. 23898-23908, 2017.
20. S. Samaneh and J. Hamelin, "Improved carbon nanostructures as a novel catalyst support in the cathode side of PEMFC: a critical review," *Carbon,* vol. 94, pp. 705-728, 2015.
21. G. Wu, K. L. More, C. M. Johnston and P. Zelenay, "High-performance electrocatalysts for oxygen reduction derived from polyaniline, iron, and cobalt," *Science,* vol. 332, no. 6028, pp. 443-447, 2011.
22. X. Sun, Y. Zhang, P. Song, J. Pan, L. Zhuang, W. Xu and W. Xing, "Fluorine-Doped Carbon Blacks: Highly Efficient Metal-Free Electrocatalysts for Oxygen Reduction Reaction," *ACS Catalysis*, vol. 3, no. 8, pp. 1726-1729, 2013.
23. Y. Tan, C. Xu, G. Chen, X. Fang, N. Zheng and Q. Xie, "Facile Synthesis of Manganese-Oxide-Containing Mesoporous Nitrogen-Doped Carbon for Efficient Oxygen Reduction," *Advanced Functional Materials,* vol. 22, no. 21, pp. 4584-4591, 2012.
24. R. Ning, C. Ge, Q. Liu, J. Tian, A. M. Asiri, K. A. Alamry, C. M. Li and X. Sun, "Hierarchically porous N-doped carbon nanoflakes: Large-scale facile synthesis and application as an oxygen reduction reaction electrocatalyst with high activity," *Carbon*, vol. 78, no. 73, pp. 60-69, 2014.
25. D. Liu, J. Zhang, C. Zhang, M. Lv, X. Zhang, H. Song, L. Du and M. Xue, "An efficient carbon catalyst supports with mesoporous graphene-like morphology," *Journal of Porous Materials*, vol. 25, no. 3, pp. 913-921, 2018.
26. P. Song, H. Wang, L. Kang, B. Ran, H. Song and R. wang, "Electrochemical nitrogen reduction to ammonia at ambient conditions on nitrogen and phosphorus co-doped porous carbon," *Chemical Communications*, vol. 55, no. 5, pp. 687-690, 2019.
27. J. Zhu, S. P. Jiang, R. Wang, K. Shi and P. K. Shen, "One-pot synthesis of a nitrogen and phosphorus-dual-doped carbon nanotube array as a highly effective electrocatalyst for the oxygen reduction reaction," *Journal of Materials Chemistry A*, vol. 2, no. 37, pp. 15448-15453, 2014.
28. H. Huang, W. Zhang, M. Li, Y. Gan, J. Chen and Y. Kuang, "Carbon nanotubes as a secondary support of a catalyst layer in a gas diffusion electrode for metal air batteries," *Journal of Colloid & Interface Science*, vol. 284, no. 2, pp. 593-599, 2005.
29. F. Xiao, X. P. Qin, M. J. Xu, S. Q. Zhu, L. L. Zhang, Y. M. Hong, S. I. Choi, Q. W. Chang, Y. Xu, X. Q. Pan and M. H. Shao, "Impact of Heat Treatment on the Electrochemical Properties of Carbon-Supported Octahedral Pt-Ni Nanoparticles," *ACS Catalysis*, vol. 9, no. 12, pp. 11189-11198, 2019.
30. Y. P. Cui, Y. R. Shang, R. X. Shi, Q. D. Che, Y. Z. Wang and P. Yang, "Effects of preparation conditions on the morphology and photoelectrochemical performances of electrospun WO_3 nanofibers," *Applied Physics a-Materials Science & Processing*, vol. 125, no. 10, pp. 724-731, 2019.
31. P.L. He X.-Y. Yu., and X. W. Lou, "Carbon-Incorporated Nickel–Cobalt Mixed Metal Phosphide Nanoboxes with Enhanced Electrocatalytic Activity for Oxygen Evolution," *Angewandte Chemie*

International Edition, vol. 56, no. 14, pp. 3897-3900, 2017.

32. G. Zhang, G. C. Wang, Y. Liu, H. J. Liu, J. H. Qu and J. H. Li, "Highly Active and Stable Catalysts of Phytic Acid-Derivative Transition Metal Phosphides for Full Water Splitting," *Journal of the American Chemical Society*, vol. 138, no. 44, pp. 14686-14693, 2016.
33. Z. H. Xiao, X. B. Huang, L. Xu, D. F. Yan, J. Huo and S. Y. Wang, "Edge-selectively phosphorus-doped few-layer graphene as an efficient metal-free electrocatalyst for the oxygen evolution reaction," *Chemical Communications*, vol. 52, no. 88, pp. 13008-13011, 2016.
34. Q. C. Xu, H. Jiang, H. X. Zhang, H. B. Jiang and C. Z. Li, "Phosphorus-driven mesoporous Co_3O_4 nanosheets with tunable oxygen vacancies for the enhanced oxygen evolution reaction," *Electrochimica Acta*, vol. 259, pp. 962-967, 2018.
35. L. Jiao, Y. X. Zhou and H. L. Jiang, "Metal-organic framework-based CoP/reduced graphene oxide: high-performance bifunctional electrocatalyst for overall water splitting," *Chemical Science*, vol. 7, no. 3, pp. 1690-1695, 2016.
36. W. Li, S. L. Zhang, Q. N. Fan, F. Z. Zhang and S. L. Xu, "Hierarchically scaffolded CoP/CoP_2 nanoparticles: controllable synthesis and their application as a well-matched bifunctional electrocatalyst for overall water splitting," *Nanoscale*, vol. 9, no. 17, pp. 5677-5685, 2017.
37. X. Li, Q. Jiang, S. Dou, L. Deng, J. Huo and S. Wang, "ZIF-67-derived Co-NC@CoP-NC nanopolyhedra as an efficient bifunctional oxygen electrocatalyst," *Journal of Materials Chemistry A*, vol. 4, no. 41, pp. 15836-15840, 2016.
38. P. Li and H. C. Zeng, "Advanced oxygen evolution catalysis by bimetallic Ni-Fe phosphide nanoparticles encapsulated in nitrogen, phosphorus, and sulphur tri-doped porous carbon," *Chemical Communications*, vol. 53, no. 44, pp. 6025-6028, 2017.
39. H. Zhong, Y. Luo, S. He, P. Tang, D. Li, N. Alonsovante and Y. Feng, "Electrocatalytic Cobalt Nanoparticles Interacting with Nitrogen-Doped Carbon Nanotube in Situ Generated from a Metal-Organic Framework for the Oxygen Reduction Reaction," *ACS Applied Materials & Interfaces*, vol. 9, no. 3, pp. 2541-2549, 2017.
40. J. Li, S. Li, Y. Tang, K. Li, L. Zhou, N. Kong, Y.Q. Lan, J.C. Bao and Z.H. Dai. "Heteroatoms ternary-doped porous carbons derived from MOFs as metal-free electrocatalysts for oxygen reduction reaction," *Scientific Reports*, vol. 4, pp. 5130, 2015.
41. C. H. Choi, S. H. Park, and S. I. Woo, "Binary and Ternary Doping of Nitrogen, Boron, and Phosphorus into Carbon for Enhancing Electrochemical Oxygen Reduction Activity," *ACS Nano*, vol.6, pp. 7084-7091, 2012.
42. J. Liang, Y. Jiao, M. Jaroniec and S. Z.Qiao, "Sulfur and Nitrogen Dual-Doped Mesoporous Graphene Electrocatalyst for Oxygen Reduction with Synergistically Enhanced Performance," *Angewandte Chemie International Edition*, vol.51, pp. 11496–11500, 2012.
43. L. Yang, X.F. Zeng, W.C. Wang and D.P. Cao. "Recent Progress in MOF-Derived, Heteroatom-Doped Porous Carbons as Highly Efficient Electrocatalysts for Oxygen Reduction Reaction in Fuel Cells, " *Advanced Functional Materials*, vol.28, pp.1704537, 2018.

44. J.L. Liu, D.D. Zhu, C.X. Guo, A. Vasileff and S.Z. Qiao, "Design Strategies toward Advanced MOF-Derived Electrocatalysts for Energy-Conversion Reactions," *Advanced Energy Materials*, vol.7, no. 23, pp.1700518, 2017.

45. E. Frbbri, M. Nachtegaal, T. Binninger, X. Cheng, B.J. Kim, J. Durst, F. Bozza, T. Graule, R. Schäublin, L. Wiles, M. Pertoso, N. Danilovic, K. E. Ayers and T.J. Schmidt, " Dynamic surface self-reconstruction is the key of highly active perovskite nano-electrocatalysts for water splitting," *Nature Materials*, vol.16, no. 9, pp. 925-931, 2017.

Figures

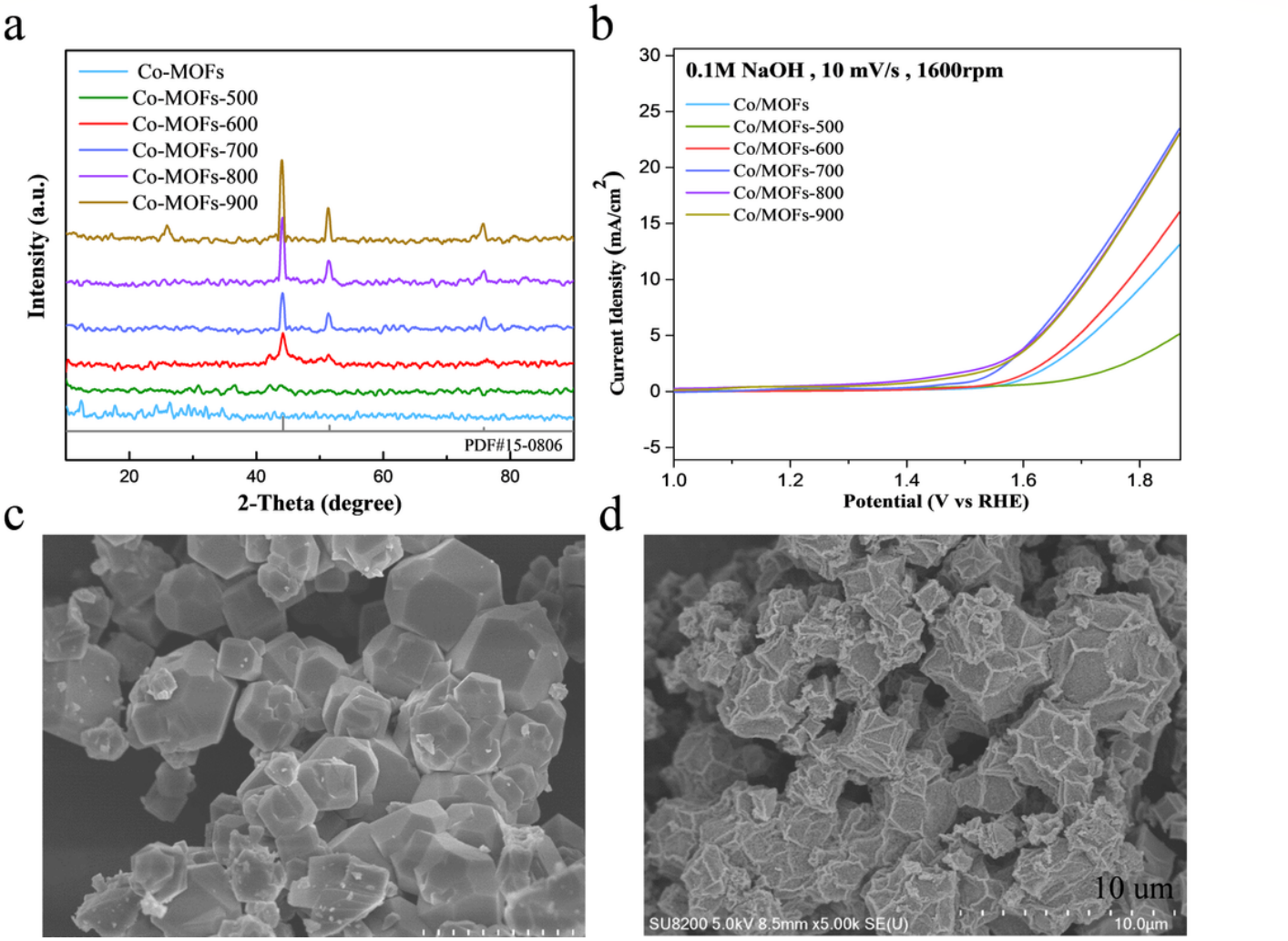

Figure 1

(a) XRD patterns of Co/MOFs samples before carbonized and carbonized at different temperatures; (b) LSV curves for the OER of Co/MOFs, Co/MOFs-500, Co/MOFs-600, Co/MOFs-700, Co/MOFs-800 and Co/MOFs-900; (c) and (d) SEM images of Co/MOFs-700 sample before and after carbonized.

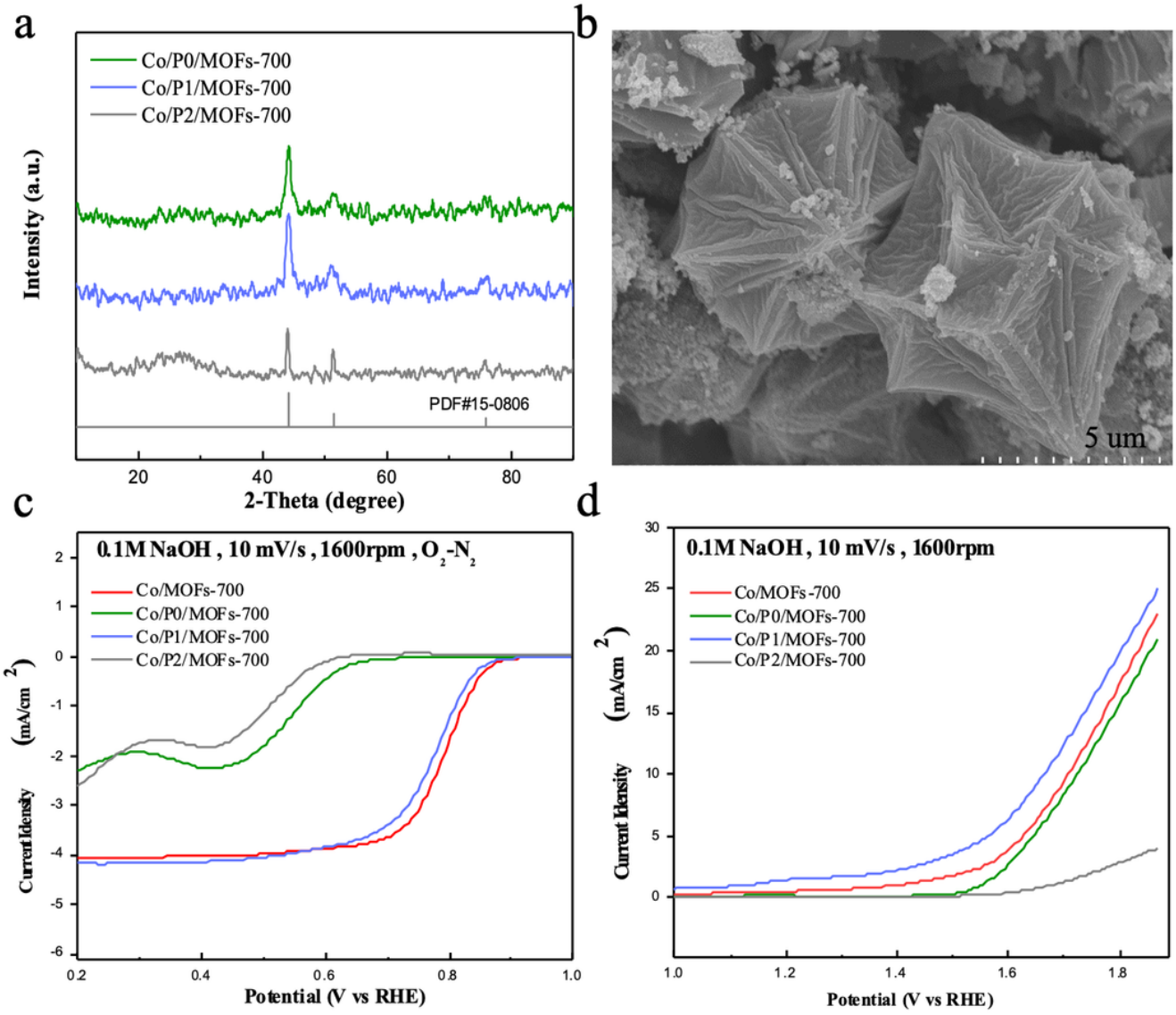

Figure 2

(a) XRD pattern of Co/P0/MOFs-700, Co/P1/MOFs-700 and Co/P2/MOFs-700; (b) SEM images of Co/P1/MOFs-700; (c) ORR polarization curves of the phosphorus-doped samples; (d) OER polarization curves of phosphorus-doped samples.

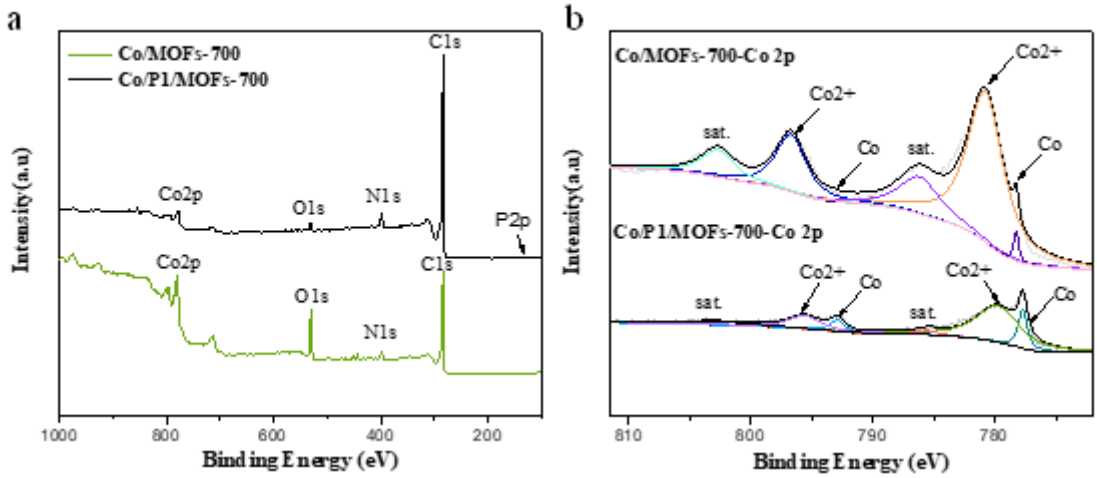

Figure 3

(a) XPS spectra survey of Co/MOFs-700 and Co/P1/MOFs-700; (b) Co 2p spectra of Co/MOFs-700 and Co/P1/MOFs-700.

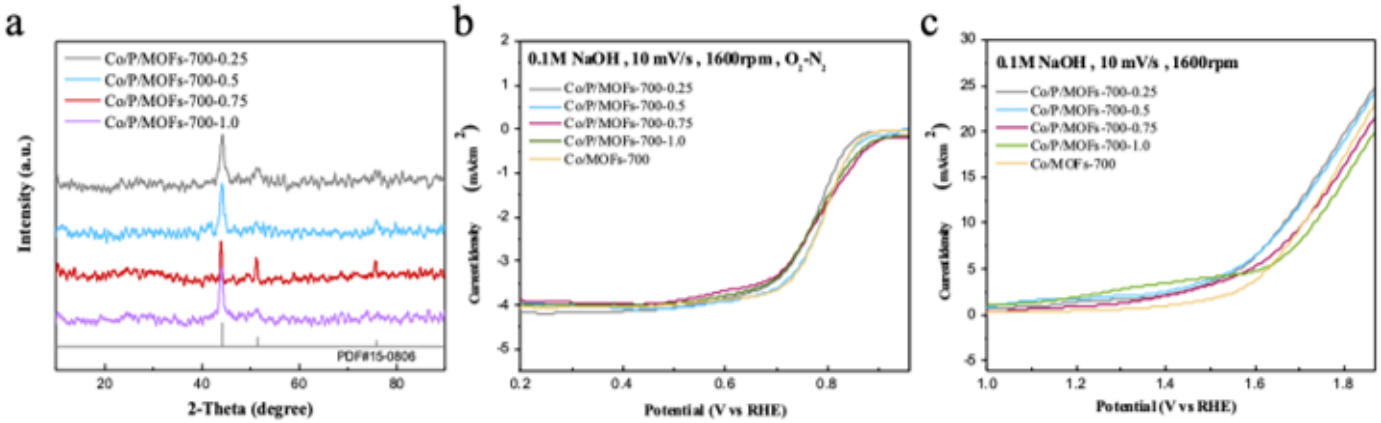

Figure 4

(a) XRD patterns of doping different content of phosphorus source into Co-MOFs; (b) and (c) ORR and OER polarization curves Co/MOFs-700, Co/P/MOFs-700-0.25, Co/P/MOFs-700-0.5, Co/P/MOFs-700-0.75 and Co/P/MOFs-700-1.0, respectively.

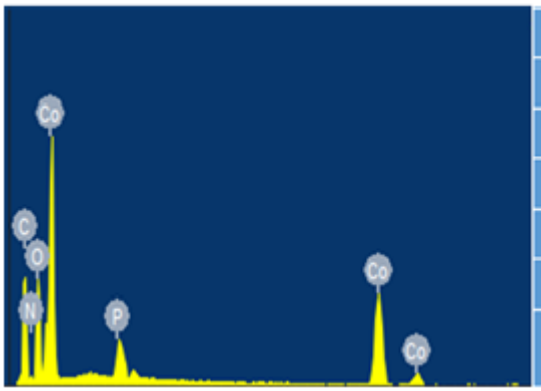

Element	Weight%	Atomic%	
C K	29.13	54.22	
N K	2.09	3.33	
O K	15.87	22.19	
P K	0.53	0.38	
Co K	52.38	19.88	
Totals	100.00		

Figure 5

EDS of Co/P/MOFs-700-0.5

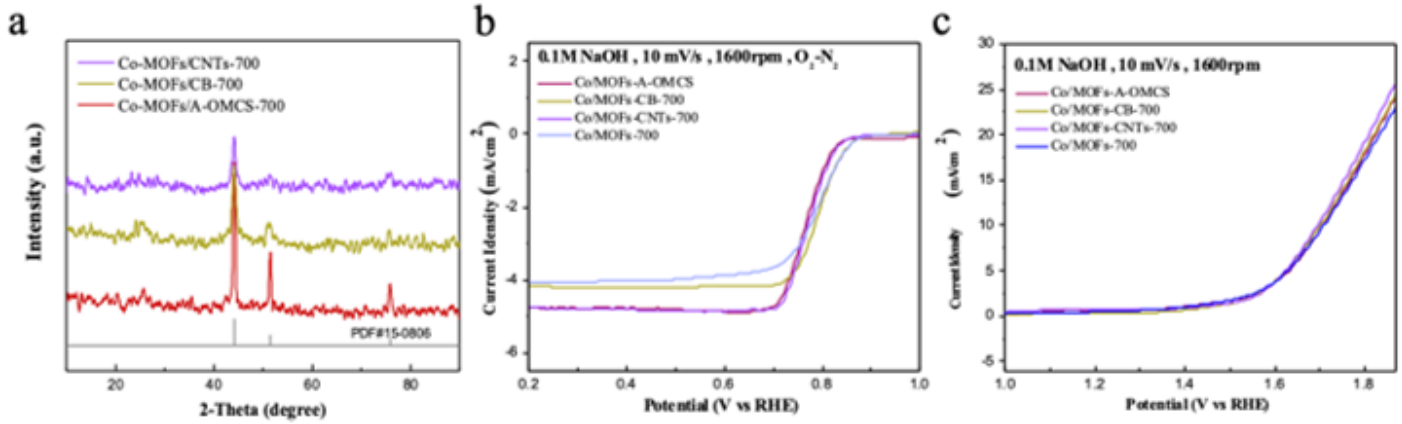

Figure 6

(a) XRD patterns of doping different content of carbon source into Co-MOFs; (b), (c) ORR and OER polarization curves OER of Co/MOFs-700、Co/MOFs-CNTs-700、Co/MOFs-A-OMCS-700 and Co/MOFs-CB-700, respectively.

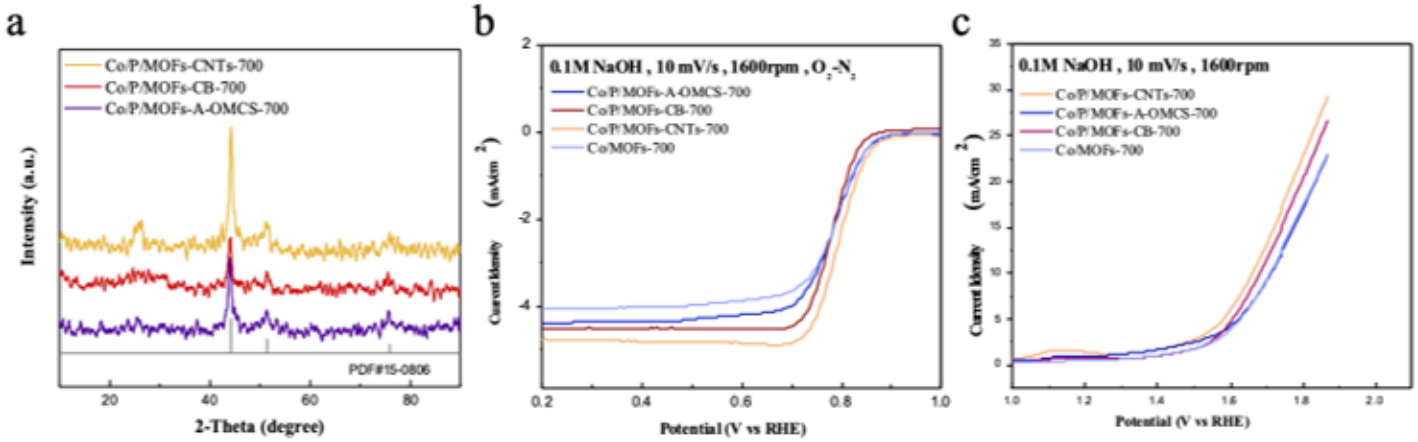

Figure 7

(a) XRD patterns of Co/P/MOFs-CNTs-700, Co/P/MOFs-A-OMCS-700 and Co/P/MOFs-CB-700; (b) and (c) ORR and OER LSV curves for the above samples, respectively.

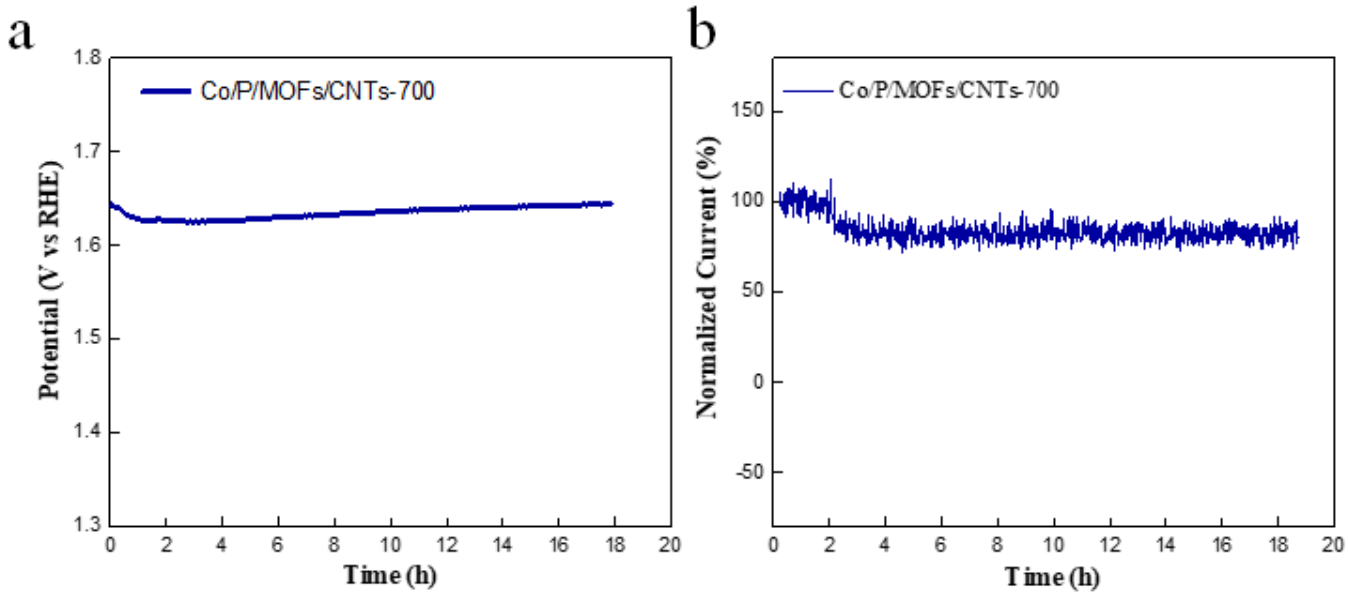

Figure 8

(a) Chronopotentiometry measurement for Co/P/MOFs-CNTs-700; (b) Chronoamperometric response of Co/P/MOFs-CNTs-700.

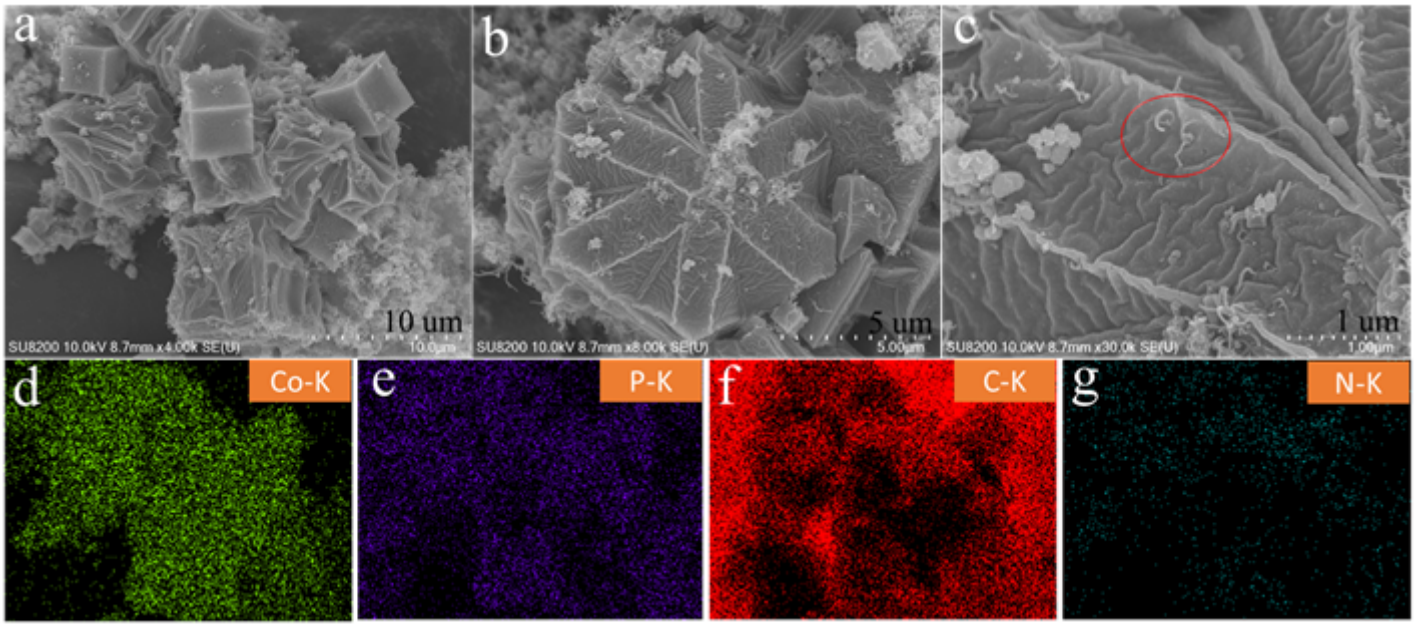

Figure 9

SEM images of Co/P/MOFs-CNTs-700 (a-c) and the corresponding elemental mapping of Co (d), P (e), C (f) and N (g), respectively

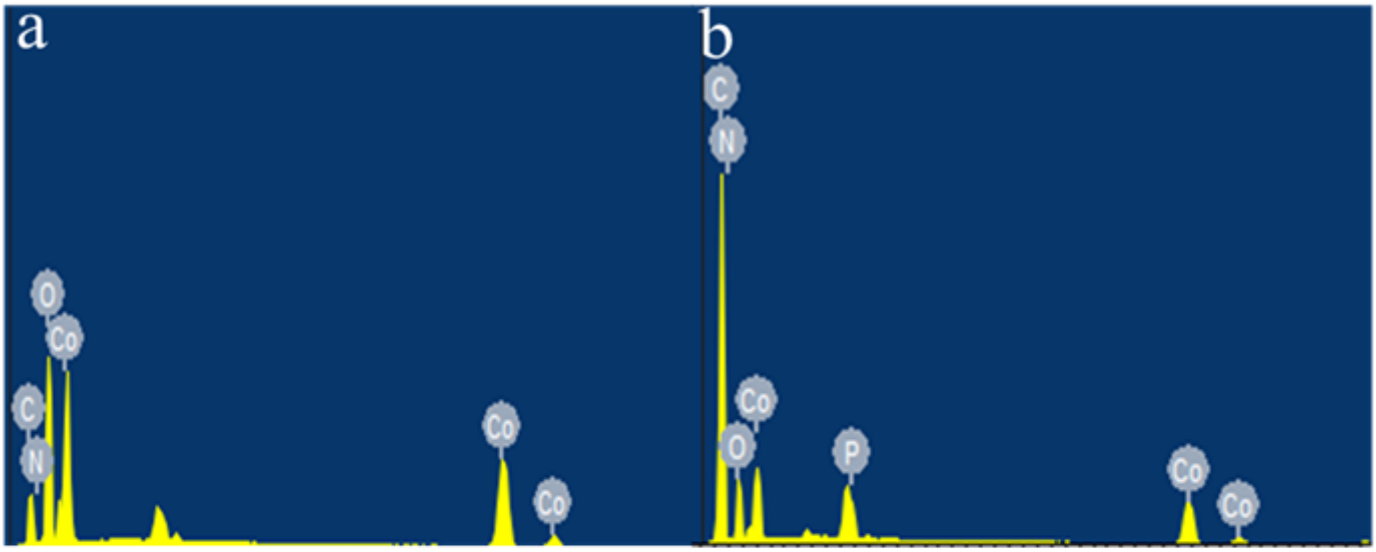

Element	Weight%	Atomic%	
C K	17.17	35.34	
N K	0.62	1.09	
O K	25.82	39.90	
Co K	56.39	23.66	
Totals	100.00		

Element	Weight%	Atomic%	
C K	59.79	78.33	
N K	0.35	0.40	
O K	14.69	14.45	
P K	0.43	0.22	
Co K	24.74	6.61	
Totals	100.00		

Figure 10

(a) and (b) EDS analysis of Co/MOFs-700 and Co/P/MOFs-CNTs-700, respectively.